

Astronomical Infrared Bands and Diffuse Interstellar Bands Both Reproduced by Hydrocarbon Pentagon-Hexagon Combined PAH Molecules

Norio Ota

Graduate school of Pure and Applied Sciences, University of Tsukuba, 1-1-1 Tennodai, Tsukuba-City Ibaraki 305-8571, Japan

This study theoretically predicts the specific Polycyclic Aromatic Hydrocarbon (PAH) molecules to reproduce both astronomically observed Infrared Bands (IR) and Diffuse Interstellar Bands (DIB). In our recent paper, we could reproduce IR by the hydrocarbon pentagon-hexagon combined PAH molecules using Density Functional Theory (DFT). Found molecules were (C₅₃H₁₈), and (C₂₃H₁₂) with two carbon pentagons among hexagon networks. Origin of DIB may come from the molecular orbital excitation. We applied Time-Dependent DFT calculation. In case of (C₅₃H₁₈), by comparing calculation with observed DIB, we found 7 coincide bands among 42 calculated bands within observed band width. For example, neutral (C₅₃H₁₈) shows calculated 577.35nm band coincide well with observed DIB at 577.95nm within 1.55nm observed band width. Mono-cation shows calculated 627.87nm correspond to observed 627.83nm, also for di-cation calculated 635.89nm to observed 635.95nm. For smaller size molecule (C₂₃H₁₂), we found 5 coincide bands, of which mono-cation shows calculated 713.92nm coincide with observed 713.80nm, di-cation shows calculated 653.27nm correlate to observed 653.21nm. By such quantum-chemical survey, we could predict specific PAH molecules floating in interstellar space.

Key words: DIB, IR, PAH, molecular orbit, TD-DFT

1. Introduction

This paper theoretically predicts background molecules to coincide with both astronomically observed infrared emission bands (IR) and Diffuse Interstellar absorbed Bands (DIB)¹⁾. In our recent paper²⁾, specific PAHs were reported to coincide well with observed IR, which were selected under the astronomical top-down material creation model³⁾ by the density functional theory (DFT) based calculation on polycyclic aromatic hydrocarbon (PAH) molecules. Obtained PAHs were (C₅₃H₁₈), (C₂₃H₁₂) and (C₁₂H₈), which has one or two pentagon hydrocarbon units among hexagon networks. In this study, we expected that those molecules may contribute again on DIB. It was supposed that DIB may come from the photoexcitation (absorption) between molecular orbitals. We tried the Time-Dependent DFT (TD-DFT) calculation.

To identify specified PAH, we did paradigm shift from the bottom-up astronomical dust creation scheme to the top-down one. Those were reviewed by A. Tielens³⁾ in 2013. Conventional bottom-up process was that few atoms create larger molecule one by one as like laboratory chemical reaction. For example, C₂ chemically reacts with C₄ to result C₆. On the other hand, the top-down creation was physical transformation of larger molecule to smaller one as like laboratory physical sputtering, for example from

C₆ to C₅ by high-speed proton attack on carbon atom. We already applied this top-down scheme to molecular vibrational IR and show successful coincidence²⁾ with well-known astronomical PAH bands in a wide wavelength from 3.2, 6.3, 7.7, 8.6, 11.2, to 12.7 micrometer^{4)·11)}. Recent review on astronomical PAHs was opened by A. Li¹²⁾ in 2020.

The Diffuse Interstellar Bands (DIB) are a large set of absorption features at a wide range of visible to infrared wavelengths to associate partly with carbon and /or hydrocarbon molecules as reviewed by T. R. Geballe¹⁾. The discovery of the first diffuse interstellar bands was made by Mary Lea Heger¹³⁾, almost 100 years ago. Until now, there observed over 500 DIBs^{14)·19)}. However, any specific molecule had not been identified yet. In 2015, four near-infrared DIBs were matched to the laboratory spectrum of singly cationic fullerene C₆₀⁺^{20)·23)}. However, others were not identified yet. This is the great mystery for the astrochemistry and molecular science.

Purpose of this study is to indicate the specific molecule to satisfy both astronomically observed IR and DIB.

2. Top-Down Scheme for Creating Interstellar Molecule

We followed astrophysical dust creation model. The first assumption is the creation of giant molecule after the death of large star. Just after star explosion, high

temperature carbon plasma was released to circumstellar space as imaged in (1) of Fig. 1. This causes cooling of plasma and collision with previously emitted dust cloud, resulting in the creation of giant carbon molecules. Nozawa et al.^{24,25} calculated the chemical composition, size distribution, and amount of dust grains formed in the ejecta of population III super novae. After 10^5 years, there may remain carbon dust with size from 1 to 10 nm, which suggests 100 to 10000 carbons giant molecule. By laboratory experiments^{26,27} and by simulation²⁸, it was confirmed that large carbon molecules would be created at a high temperature plasma condition. Those carbon molecules sometimes may react with primarily ejected hydrogen cloud, and finally transformed to large size PAHs.

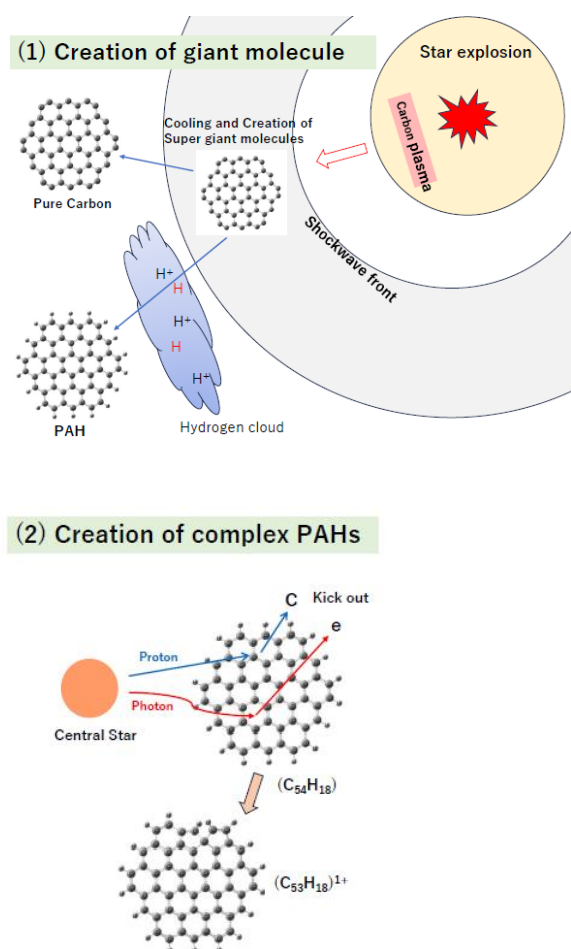


Fig. 1 (1) Image of creating giant carbon and/or PAH molecules after the star explosion. (2) Creation of pentagon-hexagon combined PAH by high-speed proton attack and high energy photon irradiation from the central star.

A capable second step would be realized around an active central star^{29,30} as shown on bottom in (2). Floating PAH would be attacked by high-speed particles as like proton and/or electrons emitted from

central star. Carbon atom in a molecule will be kicked out to result in new deformed molecule. Typical example was shown that full hexagon hydrocarbon ($C_{54}H_{18}$) will be transformed to ($C_{53}H_{18}$) having two pentagons among many hexagons. Also, central star illuminates high energy photon on those transformed PAH, which extract electron to result in the molecule to be cationic PAH as like mono-cation, di-cation and so on³⁰. Complex PAH and its family would be created by such physical top-down process.

3. Calculation Methods

In calculation, we used DFT^{31,32} and TD-DFT³⁵ with the unrestricted PBE functional^{33, 34}. We utilized the Gaussian09 software package³⁵ employing an atomic orbital 6-31G basis set³⁶. Unrestricted DFT calculation was done to have the spin dependent atomic structure. The required convergence of the root-mean-square density matrix was 10^{-8} . Based on such optimized molecular configuration, fundamental vibrational modes were calculated. This calculation also gives harmonic vibrational frequency and intensity in infrared region. To each IR spectral line, we assigned a Gaussian profile with a full width at half maximum (FWHM) of 4cm^{-1} .

For obtaining the molecular orbital excitation energy and strength, we tried TD-DFT calculation in Gaussian09 package. Excited energies were calculated simultaneously up to 14th excitations.

The scaling factor "s" between the experimental energy to the DFT calculated energy is $s=0.990$, estimated from fundamental vibration modes of coronene ($C_{24}H_{12}$) discussed by Koichi Ohno in 2011⁴². Scaling estimation in this study using PBE functional with 6-31G basis set was noted in Appendix-1 and -2.

4. Molecule Candidates from IR Study

In our previous papers^{2,30}, we tried to find specific PAH molecule under the top-down scheme. We successfully indicated specific molecule group. Typical examples were ($C_{53}H_{18}$) shown in Fig. 2 and ($C_{23}H_{12}$) in Fig. 3. Astronomically observed spectra for four different astronomical objects show general band structure, so called PAH type bands, at 3.2, 6.3, 7.7, 8.6, 11.2, and 12.7 μm . We could reproduce those bands by above molecules using DFT calculation.

In large molecule of ($C_{53}H_{18}$) in Fig. 2, charge neutral one shows 11.1 μm peak close to observed 11.2 μm band. Mono-cation reproduced four coincident bands at 3.2, 6.3, 7.6 and 8.7 μm . Di-cation calculated bands were somewhat resemble to mono-cation one.

In a small size molecule of ($C_{23}H_{12}$) in Fig. 3, di-cation shows good coincidence at 3.2, 7.7, 8.6, 11.2, and 11.6 μm . Mono-cation also presents similar behavior.

Those molecules would be candidates reproducing DIB.

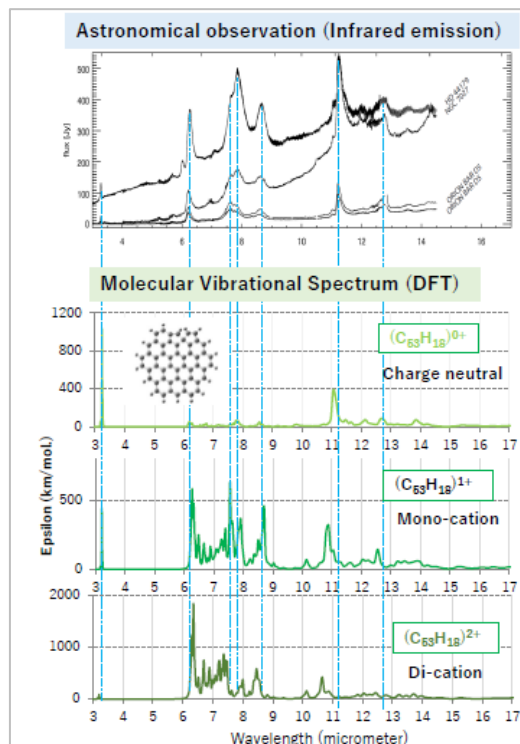


Fig. 2 Calculated IR of $(C_{53}H_{18})^{n+}$ (charge $n=0, 1$ and 2) compared with astronomically observed IRs of four different objects.

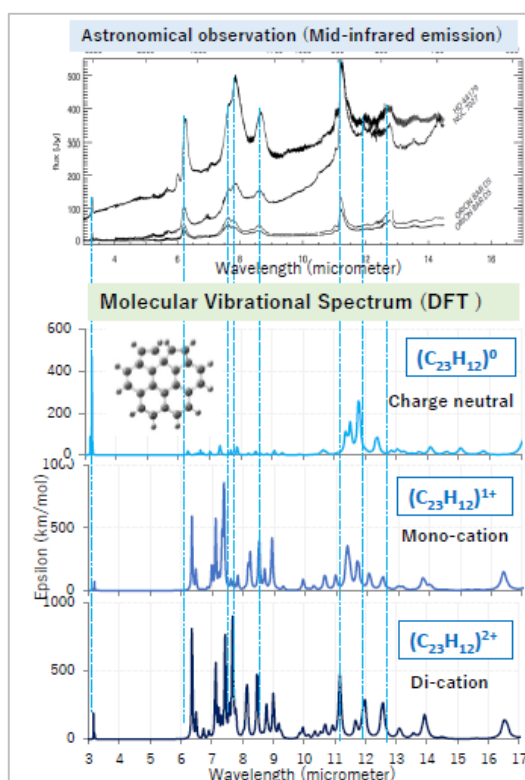


Fig. 3 Calculated IR of $(C_{23}H_{12})^{n+}$ ($n=0, 1$ and 2) compared with observed IRs.

5. Molecular Orbitals and Excitation Energy

Typical example of molecular orbital calculation was illustrated in Fig. 4 for mono-cation $(C_{53}H_{18})^{1+}$. Optimization of molecular configuration and mapping of spin density was done by DFT. In panel (a), we can see configuration with two hydrocarbon pentagons among hexagon networks. In panel (b), up-spin cloud (by red) and down-spin one (blue) was mapped. Up-spin rich arrangement was appeared around pentagon sites. By TD-DFT calculation, molecular orbital energy diagram was obtained as shown in (c). HOMO orbit was #167 for up-spin alpha bands marked by red arrow and down-spin beta bands by blue. LUMO was #168. We obtained excitation energy among those molecular orbits. Lowest one was absorption is N1 from Beta #167 (HOMO) to #168 (LUMO), which photon energy is $N1=2619\text{nm}$ in wavelength. Second one was $N2=1567\text{nm}$ from Beta#166 to #168. Third one was $N3=1066\text{nm}$. Other higher excitation energy was calculated until 14th. Molecular orbits were illustrated in (d) for Beta HOMO and LUMO, where orange cloud show plus-sign orbit and green cloud for anti-sign one. LUMO orbit became complex structure than HOMO.

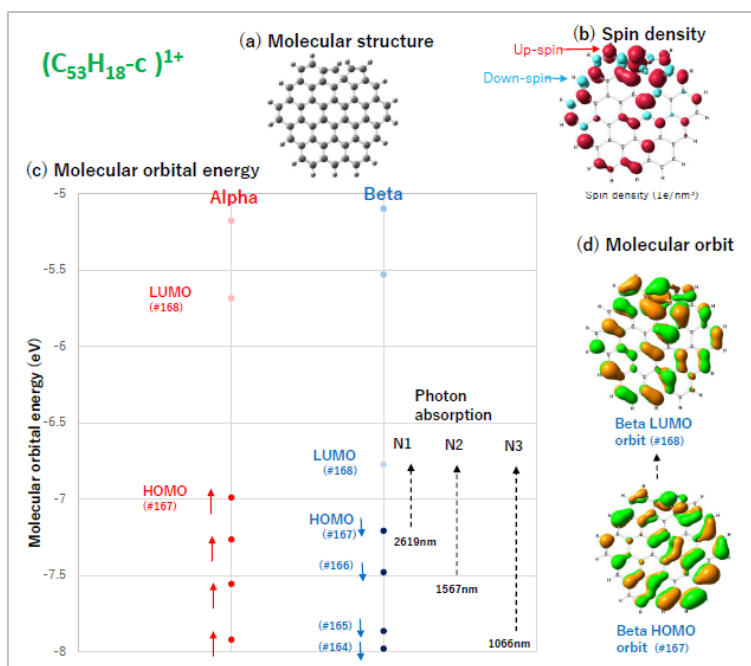


Fig. 4 Configuration of $(C_{53}H_{18})^{1+}$ in (a), and spin density in (b). TD-DFT calculated molecular orbital energy diagram was shown in (c) for up-spin Alpha bands by red arrows and down spin Beta one by blue. Excitation energy was calculated as N1, N2, N3 up to N14. Molecular orbits were mapped in (d).

Table 1, TD-DFT calculated molecular excitation bands of $(C_{53}H_{18})^{n+}$ ($n=0, +1, +2$) on left by green columns compared with observed DIB bands ³⁸⁾ by blue. Yellow colored column is coincided band with observed DIB within observed width of FWHM.

TD-DFT Calculation (This study) $S=0.990$			DIB Observation by Jenniskens et al. ³⁸⁾			
Excitation number	Wavelength (nm)	Oscillating Strength ($\times 10E-4$)	Wavelength (nm)	FWHM (nm)	W/EB-V	
$(C_{53}H_{18})$ Charge neutral 	N1	761.57	-485	758.56	0.09	0.01
	N2	679.67	-107	679.53	0.09	0.01
	N3	577.35	-756	577.95	1.55	0.08
	N4	558.80	-960	554.50	0.08	0.02
	N5	534.73	-595	536.21	0.60	0.08
	N6	505.57	-83	510.97	1.18	0.27
	N7	491.95	-601	488.18	1.97	0.61
	N8	474.24	-797	476.17	2.53	0.45
	N9	469.43	-60	466.55	0.40	0.17
	N10	458.11	-1268	459.50	2.80	0.45
	N11	452.99	-2095	450.18	0.25	0.20
	N12	441.50	-165	442.89	1.23	2.23
	N13	436.00	-273	n (not listed)		
	N14	431.17	-2304	n		
$(C_{53}H_{18})^{1+}$ Mono-cation	N1	2619.26	-46	x (out of list)		
	N2	1567.07	-171	x		
	N3	1066.79	-195	x		
	N4	977.05	-131	x		
	N5	915.60	-234	x		
	N6	822.67	-195	n		
	N7	795.42	-40	792.78	1.50	0.43
	N8	710.27	-104	710.60	0.25	0.04
	N9	683.25	-21	682.72	0.10	0.02
	N10	659.99	-36	659.14	0.56	0.09
	N11	633.54	-133	633.04	0.10	0.02
	N12	627.87	-70	627.83	0.06	0.02
	N13	622.50	-132	622.36	0.05	0.01
	N14	613.19	-459	613.98	0.09	0.01
$(C_{53}H_{18})^{2+}$ Di-cation	N1	2786.96	-62	x		
	N2	1530.90	-221	x		
	N3	1012.13	-594	x		
	N4	916.31	-279	x		
	N5	851.67	-218	853.08	0.17	0.07
	N6	684.87	-481	684.33	0.12	0.03
	N7	649.71	-45	649.78	0.05	0.01
	N8	635.89	-631	635.95	3.73	0.54
	N9	615.45	-379	617.72	2.30	0.77
	N10	589.42	-1677	585.40	0.18	0.02
	N11	571.41	-464	570.48	0.66	0.08
	N12	523.41	-311	n		
	N13	505.67	-1581	503.91	1.79	0.28
	N14	500.39	-298	496.97	3.37	0.50

Table 2, Molecular orbital excitation energy of $(C_{23}H_{12})^{n+}$ (left green column) compared with observed DIB bands (right green column).

TD-DFT Calculation (This study) $S=0.990$				DIB Observation by Jenniskens et al. ³⁸⁾		
Excitation number	Wavelength (nm)	Oscillating strength ($\times 10E-4$)	Wavelength (nm)	FWHM (nm)	W/EB-V	
$(C_{23}H_{12})^0$ Charge neutral 	N1	488.16	-37	488.18	1.96	0.610
	N2	449.16	-13	450.18	0.25	0.200
	N3	397.83	-368	x		
	N4	396.48	-287	x		
	N5	360.86	-109	x		
	N6	353.96	-747	x		
	N7	343.66	-47	x		
	N8	318.91	-99	x		
	N9	307.18	-376	x		
	N10	300.82	-2695	x		
	N11	290.71	-21	x		
	N12	290.43	-296	x		
	N13	290.28	-154	x		
	N14	280.89	-1005	x		
$(C_{23}H_{12})^{1+}$ Mono-cation	N1	1932.19	-77	x		
	N2	1206.18	-105	x		
	N3	713.92	-274	713.80	0.35	0.05
	N4	608.23	-43	608.98	0.08	0.02
	N5	537.27	-6	536.21	0.60	0.08
	N6	524.39	-9	n		
	N7	506.84	-1	n		
	N8	492.60	-4	n		
	N9	478.18	-16	478.01	0.15	0.06
	N10	476.98	-97	476.17	2.53	0.62
	N11	426.37	-1	n		
	N12	422.44	-12	n		
	N13	414.21	-417	n		
	N14	407.14	-1	n		
$(C_{23}H_{12})^{2+}$ Di-cation	N1	2144.08	-62	x		
	N2	1299.37	-106	x		
	N3	653.27	-357	653.21	1.72	0.66
	N4	552.81	-106	553.70	2.26	0.29
	N5	500.72	-45	503.91	1.79	0.284
	N6	468.98	-32	466.54	0.4	0.17
	N7	435.43	-549	n		
	N8	428.93	-73	n		
	N9	419.30	-54	n		
	N10	402.89	-20	n		
	N11	382.14	-32	x		
	N12	362.56	-1805	x		
	N13	353.38	-410	x		
	N14	336.84	-1732	x		

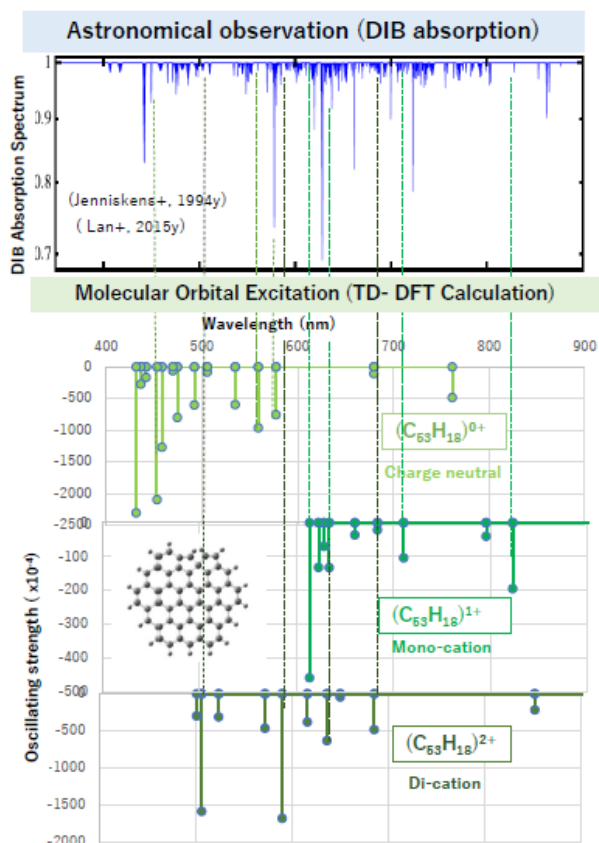


Fig. 6 Calculated molecular orbital excitation for $(C_{53}H_{18})^{n+}$ ($n=0, 1$ and 2) by different green lines compared with observed DIB bands by blue lines.

8, Small Size Molecule: $(C_{23}H_{12})^{n+}$

Molecular orbital excitation of small size molecule $(C_{23}H_{12})^{n+}$ ($n=0, 1$ and 2) are shown in Fig. 7 for every charged state. Detailed comparison with observation³⁸⁾ was listed in Table 2.

In case of charge neutral, there is one coincident band of N1 at 488.16nm coincide very well with observed 488.18nm with difference only 0.02nm and within width of 1.96nm FWHM. Shorter wavelength excitation less than 400nm were not listed in the Jenniskens observation list³⁸⁾. Future observation is necessary in violet wavelength region for small size molecules.

Mono-cation show 2 coincident bands. Calculated N3 at 713.92nm reproduces well observed 713.80nm band within 0.35nm FWHM. Also, N10 at 476.98nm correspond to observed 476.17nm within 2.53nm FWHM.

Di-cation show N3 band at 653.27nm close to observed 653.21nm within 1.72nm FWHM. Also, N4 at 552.81nm was close to observed 553.70nm.

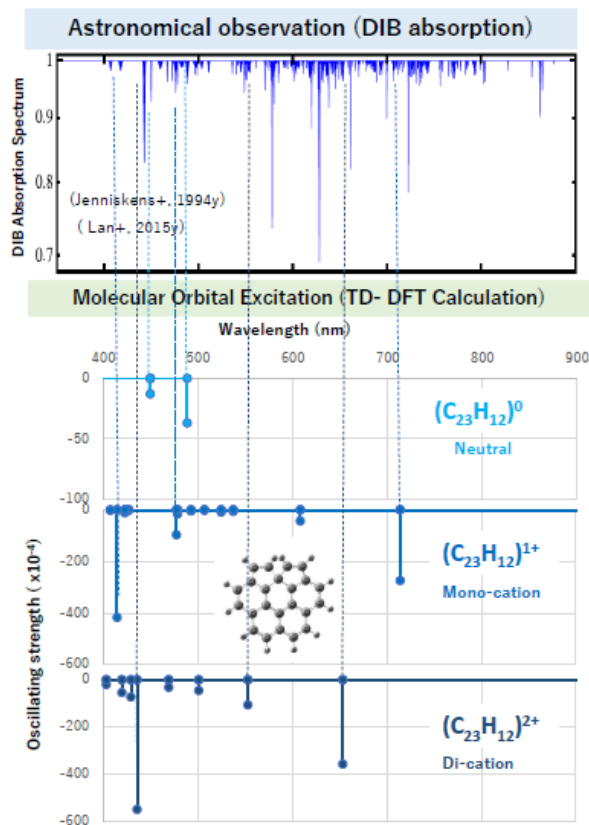


Fig. 7 Calculated molecular orbital excitation of $(C_{23}H_{12})^{n+}$ ($n=0, 1, 2$) compared with observed DIB bands.

9. Conclusion

Purpose of this study is to indicate specific PAH molecules to coincide both astronomically observed IR and DIB bands by calculation.

- (1) Under astronomical top-down material creation scheme, we have found the hydrocarbon pentagon-hexagon combined PAH molecules by comparing astronomically observed IR and DFT obtained molecular vibrational spectrum. Molecules were $(C_{53}H_{18})$ and $(C_{23}H_{12})$, which reproducing well, so called PAH type IR bands, at 3.2, 6.3, 7.7, 8.6, 11.2, and 12.7 μ m.
- (2) Origin of DIB may come from the molecular orbital excitation from those molecules. We applied Time-Dependent DFT calculation.
- (3) In case of $(C_{53}H_{18})$, we found 7 coincide bands among 42 calculated bands within an accuracy of observed FWHM. For example, neutral $(C_{53}H_{18})$ shows calculated 577.35nm band coincide well with observed DIB at 577.95nm within observed 1.55nm FWHM. Mono-cation of $(C_{53}H_{18})$ show one coincident band at 627.87nm correspond to observed 627.83nm. Di-cation also shows two good coincident bands at 635.89, 615.45 and 505.67nm

related to 635.95, 617.72 and 503.91nm.

- (4) For small molecule ($C_{23}H_{12}$), we found 5 coincide bands among 42 calculated bands. Typical example was di-cation molecule's excitation number N3 at 653.27nm coincide well with observed 653.21nm within 1.72nm FWHM.

By such quantum-chemistry survey for reproducing both IR and DIB, we could predict specified PAH molecules floating in interstellar space.

Acknowledgement

We would like to say great thanks to Prof. Aigen Li of Univ. Missouri for the important suggestions, also thanks to Dr. Christiaan Boersma of NASA Ames Research to give us astronomical IR data. We like to say special thanks to the excellent review paper by Dr. T.R. Geballe.

References

- 1) T. R. Geballe: J. of Phys.: Conference Series **728**, 062005 (2016)
- 2) N. Ota, A. Li and L. Nemes: J. Mag. Soc. Japan **45**, 86 (2021).
- 3) A. Tielens: Rev. Mod. Phys. **85**, 1021 (2013)
- 4) J. Oomens: *In PAHs and the Universe: A Symposium to Celebrate the 25th Anniversary of the PAH Hypothesis*, EAS Publications Series (2011)
- 5) C. Boersma, J. Bregman, and L. Allamandola: *ApJ* **769**, 117 (2013).
- 6) C. Moutou, K. Sellgren, L. Verstraete, and A. L'eger: *A & A*, **347**, 949 (1999).
- 7) E. Peeters, S. Hony, C. van Kerckhoven, et al.: *A&A*, **390**, 1089 (2002).
- 8) L.Armus, V.Charmandaris, J.Bernard-Salas, *ApJ*, **656**,148 (2007).
- 9) J. Smith, B. Draine, A. Dale, et al.: *ApJ* **656**, 770 (2007).
- 10) K. Sellgren, K. Uchida and M. Werner: *ApJ* **659**, 1338 (2007).
- 11) A. Ricca, C. W. Bauschlicher, C. Boersma, A.Tielens & L. J. Allamandola: *ApJ*, 754, 75 (2012).
- 12) A. Li: *Nature Astronomy*, **4**, 339 (2020).
- 13) M. L. Heger: *Lick Obs. Bull.* **10** 146 (1922)
- 14) G. P. Zwet and L. J. Allamandola: *Astron. Astrophys.* **146** 76 (1985)
- 15) A. Leger and L. D'Hendecourt: *Astron. Astrophys.* **146** 81 (1985)
- 16) M. K. Crawford, A. Tielens and L. J. Allamandola: *Astrophys. J.* **293** L45 (1985)
- 17) H. W. Kroto: *Science* **242** 1139 (1988)
- 18) A. L'eger, L. D'Hendecourt, L. Verstraete L and W. Schmidt: *Astron. Astrophys.* **203** 145 (1988)
- 19) A. Webster: *Mon. Not. R. Astron. Soc.* **263** 385 (1933)
- 20) J. Fulara, M. Jakobi and J. Maier: *Chem. Phys. Lett* **211** 227 (1933)
- 21) B. H. Foing and P. Ehrenfreund: *Nature* **369** 296 (1994)
- 22) B. H. Foing and P. Ehrenfreund: *Astron. Astrophys.* **319** L59 (1977)
- 23) E. K. Campbell, M. Holz, D. Gerlich and J. P. Maier: *Nature* **523** 322 (2015)
- 24) T. Nozawa, T. Kozasa, H. Umeda, K. Maeda & K. Nomoto: *ApJ*, 598,785 (2003)
- 25) T. Nozawa and T. Kozasa: *The Astrophysical Journal*, **648**, 435 (2006)
- 26) L. Nemes, A. Keszler, J. Hornkohl, and C. Parigger: *Applied Optics*, **44-18**, 3661 (2005).
- 27) L. Nemes, E. Brown, S. C. Yang, U. Hommerich: *Spectrochimica Acta Part A, Molecular and Biomolecular Spectroscopy*, **170**, 145 (2017).
- 28) N. Patra, P. Kr'all, and H. R. Sadeghpour: *The Astrophysical Journal*, **785**, 6 (2014)
- 29) J. Y. Seok and A. Li: *ApJ*, **835**, 291 (2017).
- 30) N. Ota and A. Li: *arXiv.org* 2303.05645 (2023)
- 31) P. Hohenberg and W. Kohn: *Phys. Rev.*, **136**, B864 (1964).
- 32) W. Kohn and L. Sham: *Phys. Rev.*, **140**, A1133(1965).
- 33) Perdew, J. P.; Burke, K.; Ernzerhof, M. *Phys. Rev. Lett.* 1996,77, 3865–3868 (1996)
- 34) Huan Wang, Youjun He, Yongfang Li and Hongmei Su: *Phys. Chem. A* 2012, 116, 255–262 (2012)
- 35) M. Frisch, G. Trucks, H. Schlegel et al: Gaussian 09 package software, Gaussian Inc. Wallington CT USA (2009).
- 36) R. Ditchfield, W. Hehre and J. Pople: *J. Chem. Phys.*, **54**,724(1971).
- 37) T. Lan, B. Menard and G. Zhu: *Mon. Not. R. Astron. Soc.* **452** 3629 (2015)
- 38) P. Jenniskens and F. Desert: 1994 *Astron. Astrophys. Suppl. Series* **106** 39 (1994)
- 39) M. G. Rawlings, A. J. Adamson, C. C. M. Marshall and P. J. Sarre: *MNRAS* **485**, 3398–3401 (2019)
- 40) T. Geballe, F. Najarro, D. Figer, B. Schlegelmilch, and D. de la Fuente: *Nature* **479** 200E (2011).
- 41) P. Sarre, J. Miles, T. Kerr, R. Hibbins, S. Fossey and W. Somerville: *Mon. Not. R. Astron. Soc.* **277** L41 (1995)

- 42) K. Ohno: Toyota Research Report **64**, 53 (2011),
<http://www.toyotariken.jp/activities/64/05ono.pdf>
 /

Appendix-1

Comparison of Molecular vibrational energy for coronene ($C_{24}H_{12}$). Left side blue column show laboratory experimental wavenumbers in cm^{-1} discussed by Koichi. Ohno⁴²⁾. Green column table was DFT calculated values under PBE/PBE functionals and 6-31G basis set in this study.

Molecular Vibration Energy (cm^{-1})		Symmetry	Vibrational mode number
Laboratory Experiment	DFT Calculation PBE/PBE 6-31G		
363.0	367.2	e2g	number-10, 11
470.6	478.5	a1g	17
771.0	778.7	e1u	36
992.3	998.7	e2g	52, 53
1137.0	1149.9	e1u	55, 56
1166.7	1178.4	e2g	59, 60
1236.7	1253.8	e2g	66, 67
1317.0	1328.9	e1u	68, 69
1370.0	1393.6	a1g	71
1401.7	1418.9	e2g	72, 73
1431.6	1461.4	e2g	77, 78
1439.6	1465.1	e2g	79, 80
1505.0	1515.8	e1u	82, 83
1603.0	1612.6	a1g	86
1620.0	1628.2	e1u	89, 90

Authors Profile : Norio Ota, PhD. (太田憲雄)
 Magnetic materials and physics, Astrochemistry,
 Honorary member of the Magnetics Society of Japan,
 2010-2021: Senior Professor, Univ. of Tsukuba, Japan.
 2003-2011: Exec. Chief Engineer, Hitachi Maxell Ltd.
<https://www.researchgate.net/profile/Norio-Ota-Or-Ohta>



Appendix-2

Scaling constant $s=0.990$ in this study obtained by comparison of molecular vibrational energy noted on Appendix 1.

